JOURNAL OF MATERIALS SCIENCE 22 (1987) 2987–2992

TEM study of reaction-sintered zirconia–mullite composites with CaO and MgO additions

P. MIRANZO, P. PENA, S. DE AZA, J. S. MOYA
Instituto de Cerámica y Vidrio, CSIC Arganda, Madrid, Spain
J. Ma RINCON*, G. THOMAS
Materials Science and Mineral Engineering, University of California, Berkeley, California, USA

The microstructural and phase evolution, which leads to final zirconia-mullite tough ceramic composites by using reaction sintering of zircon-alumina mixtures with MgO and CaO as additives, has been investigated by electron microscopy and microanalysis. The results confirm that the reaction, in a first stage, produces zirconia inside an amorphous matrix as well as saphirine and spinel for MgO and anorthite for CaO additions respectively. Finally the glassy phase distribution, the mechanical behaviour and the microstructure of the final reaction sintered compacts are comparatively discussed.

1. Introduction

The reaction sintering of zircon/alumina mixtures is one route for producing mullite–zirconia tough composites, following a conventional ceramic processing [1, 2]. In previous work [3, 4] it has been shown that additions of CaO and MgO increase the reaction-sintering process, and decrease the final sintering temperature by the appearance of a transitory liquid phase. This liquid is present during sintering and provides the same types of densification driving forces as for liquid-phase sintering, but the liquid either changes composition or disappears as the sintering process progresses or after it is completed. Because the liquid phase is consumed in the reaction, the final material can have a good high-temperature properties and, in some cases, can even be used at temperatures above the sintering temperature.

The aim of the present work was to study the microstructure development as well as the appearance and microchemistry of the different phases during the reaction-sintering process for two selected MgO- and CaO-containing composites.

The bend strength (σ_f) and the critical stress intensity factor (K_{IC}) values are discussed comparatively for these two composites.

2. Materials and methods

Taking into account the information supplied by the quaternary systems ZrO_2–Al_2O_3–SiO_2–MgO and ZrO_2–Al_2O_3–SiO_2–CaO [3–5], two compositions with the following molar proportions: $2ZrSiO_4/4Al_2O_3/MgO$ and $4ZrSiO_4/4Al_2O_3/CaO$, were studied. The formulated compositions are located in the compatibility planes ZrO_2–$Al_6Si_2O_{13}$–$MgAl_2O_4$ and ZrO_2–$Al_6Si_2O_{13}$–$CaAl_2Si_2O_8$ where the invariant points are 1450 and 1440° C, respectively. In this way, reaction sintering takes place according to the following equations:

$$2ZrSiO_4 + 4Al_2O_3 + MgO \rightarrow \underset{\text{zircon}}{2ZrO_2} + \underset{\text{mullite}}{Al_6Si_2O_{13}} + \underset{\text{spinel}}{MgAl_2O_4} \quad (1)$$

$$4ZrSiO_4 + 4Al_2O_3 + CaO \rightarrow 4ZrO_2 + Al_6Si_2O_{13} + \underset{\text{anorthite}}{CaAl_2Si_2O_8} \quad (2)$$

A very fine (1 to 3 μm average grain size) zircon (Zircon opacifier Quiminsa S.A., Spain), low-sodium Al_2O_3 (Fluka AG, Buchs SG, Switzerland) (99.998% purity) and $CaCO_3$ (E. Merck, Darmstadt, FRG) or MgO, prepared from magnesium metal [4], were used; the powders were homogenized by attrition milling in isopropyl alcohol medium for 1 h. Subsequently, the powders were isostatically pressed (Nat. Forge Europe. 60.000 PSI, no. S02814) at 200 MPa and fired for different times at 1425 and 1450° C.

The microstructure of the samples was studied by scanning electron microscopy (ETEC-Siemens) (SEM) on polished surfaces thermally etched at 1350° C, 1 h, and by transmission electron microscopy (Philips EM400 TEM/SEM) (TEM) on specimens prepared by wafering, grinding and argon-ion bombardment. Spectra at 100 kV were acquired from the TEM procedure (40 nm probe diameter) (Kevex Si (Li) detector and analytical spectrometer for X-ray analysis) and quantitative analyses were performed according to the Cliff–Lorimer method [6]. Standard specimens were used to obtain calibration factors, i.e. pure mullite (Balkowski International), zircon, a synthetic gehlenite and spinel (Balkowski International). The factors were $K_{AlSi} = 1.04 \pm 0.05$, $K_{ZrSi} = 2.3 \pm 0.1$, $K_{CaSi} = 1.0 \pm 0.1$, $K_{MgSi} = 1.2 \pm 0.1$.

The toughness, K_{IC}, and strength, σ_f, were deter-

* *Permanent address:* Instituto de Cerámica y Vidrio, CSIC, Madrid, Spain.

0022–2461/87 $03.00 + .12

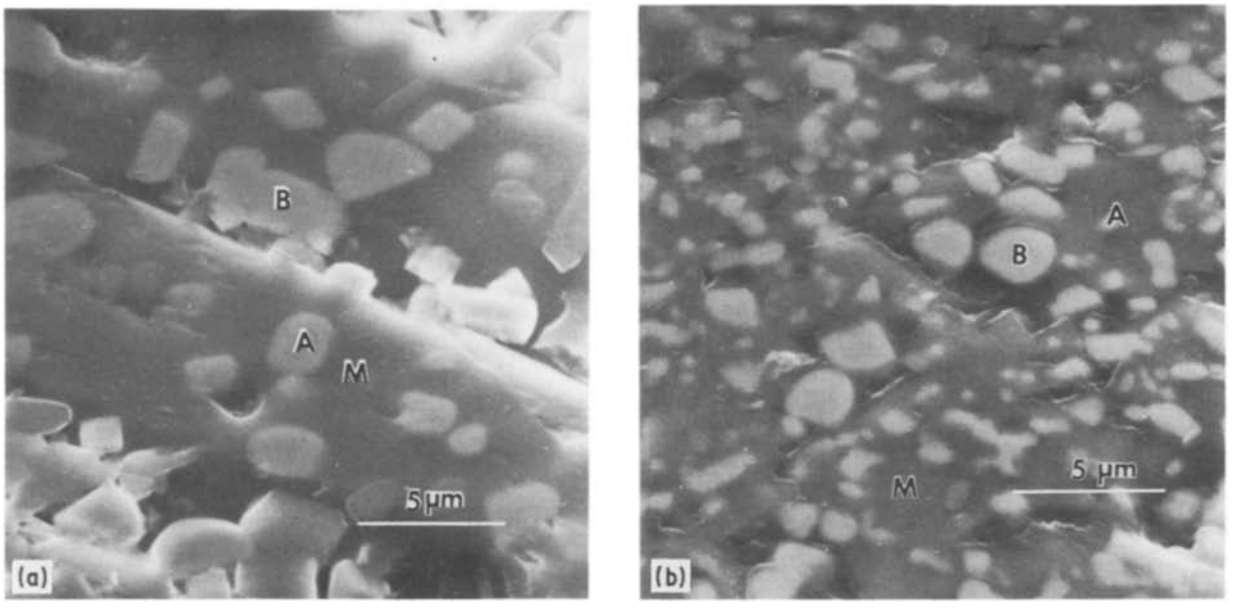

Figure 1 Scanning electron micrographs of (a) MgO-containing sample after 1.5 h at 1450° C, and (b) CaO-containing sample after 2 h at 1450° C. A, intragranular-ZrO_2; B, intergranular-ZrO_2; M, mullite.

mined by indentation and three-point bend methods, respectively.

3. Results and discussion

According to previous papers [3, 4], the reaction sintering of $ZrSiO_4/Al_2O_3/XO$ powders (XO = MgO or CaO) goes through a series of chemical reactions with one or more intermediate compounds and transient liquids before the final stable compounds are formed. These transitory phases appear at temperatures lower than those corresponding to the invariant points where ZrO_2–$Al_6Si_2O_{13}$–$MgAl_2O_4$ and ZrO_2–$Al_6Si_2O_{13}$–$CaAl_2Si_2O_8$ coexist.

Fig. 1 exhibits a general look of the microstructure of the MgO and CaO samples after sintering at 1450° C for 1.5 and 2 h, respectively. In these compacts it is possible to distinguish two kinds of zirconia particles: (a) intragranular round ZrO_2 particles inside mullite grains, and (b) intergranular sharp-edged ZrO_2 particles located between the mullite grains, as reported in previous work [3, 4].

Microtwinned intergranular ZrO_2 grains are observed by TEM in all the samples studied (Fig. 2a). Twinning reduces the shape change which accompanies the martensitic phase transformation (t-ZrO_2 → m-ZrO_2), through a proper orientation of the crystallographic axes of the microtwinned regions. In Fig. 2b a monoclinic intragranular-ZrO_2 grain, which was probably transformed during the TEM test, is shown. In this figure the stress lines produced in the mullite matrix because of the t-ZrO_2 → m-ZrO_2 transformation are observed.

The intragranular ZrO_2 particle size distributions measured on transmission electron micrographs in CaO and MgO-samples heated at 1450° C for 2 and 1.5 h, respectively, are shown in Fig. 3. The average grain sizes for both intra- and intergranular (determined on scanning electron micrographs) ZrO_2 particles are 0.30(0.08) (standard deviation of the log distribution) μm and 1.3(0.7) μm, respectively for CaO sample and 0.29(0.07) μm and 1.3(0.6) μm for MgO sample.

Many intergranular-ZrO_2 grains coarsen by coalescence in the presence of a liquid phase (Fig. 2a). The orientation of the crystallographic *a* and *c* axes of the microtwinned regions in the intergranular ZrO_2 grains are perpendicular to them. This phenomenon, observed in many clustered grains, will require further investigation in order to clarify the ultimate reason for this singular crystallographic ordering.

It has been observed by TEM in the mullite/ZrO_2 composites that the intergranular-ZrO_2 and the anorthite as well as the spinel grains are normally located close to the glassy phase regions (Fig. 4) while the mullite–mullite grain boundaries are generally glass free. Evidence of this fact is the frequent low-angle grain boundary dislocations (Fig. 2) noted at mullite–mullite interfaces, which are related to the absence of amorphous phase. In both samples, small Al_2O_3 crystals occluded inside mullite grains are detected (Fig. 5).

Both kinds of ZrO_2-particles (inter and intra) show solid solutions of Al_2O_3 and SiO_2 (3 to 5 wt % Al_2O_3 and 6 to 8 wt % SiO_2), while the mullite contains a small amount of ZrO_2 (2 wt %). No significant solid solution of CaO and MgO in mullite and ZrO_2 (according to the previous results of the present authors [5]) was noticed.

In an MgO sample treated at 1425° C the intermediate compound, saphirine, was observed by TEM and EDX (Fig. 6). This phase is associated with the presence of spinel and transitory glassy phase. Saphirine and spinel crystals have a composition close to the stoichiometric one; and the glassy phase close to these crystals has a composition of (wt %) 29.9 Al_2O_3; 56.5SiO_2; 5.7ZrO_2 and 7.9 MgO.

In the CaO sample treated at 1425° C, anorthite crystals with a composition similar to the stoichiometric one, appear frequently showing in all cases twins as observed in feldspar crystals (Fig. 4). Different

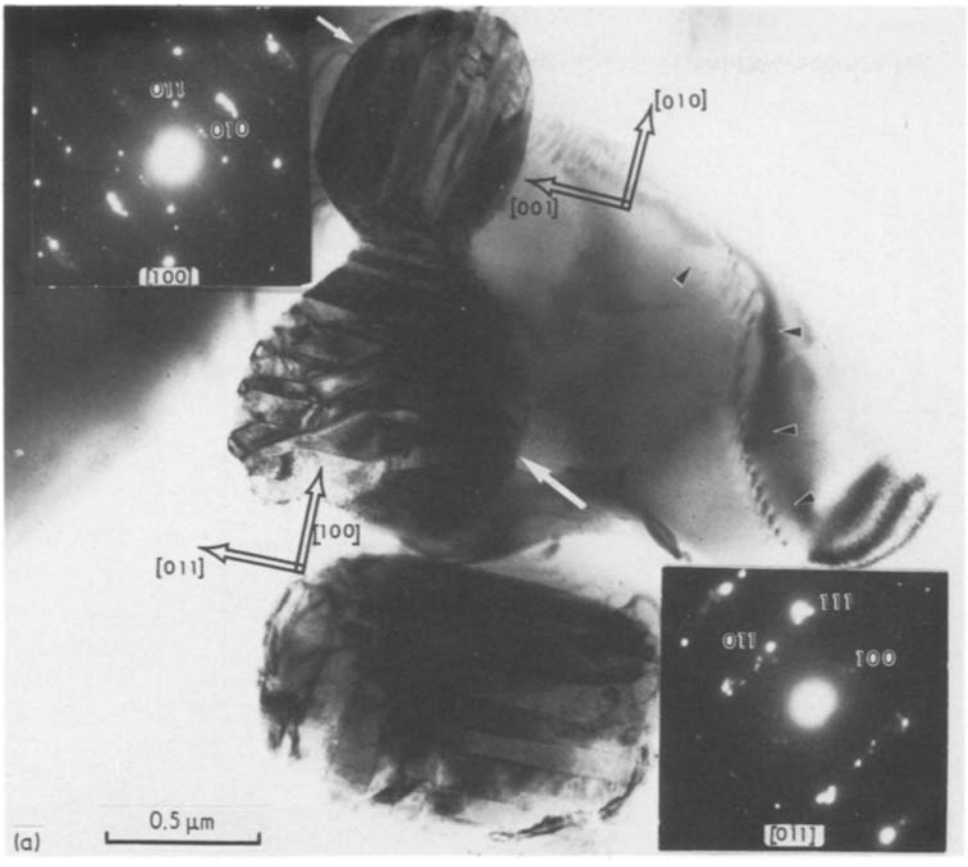

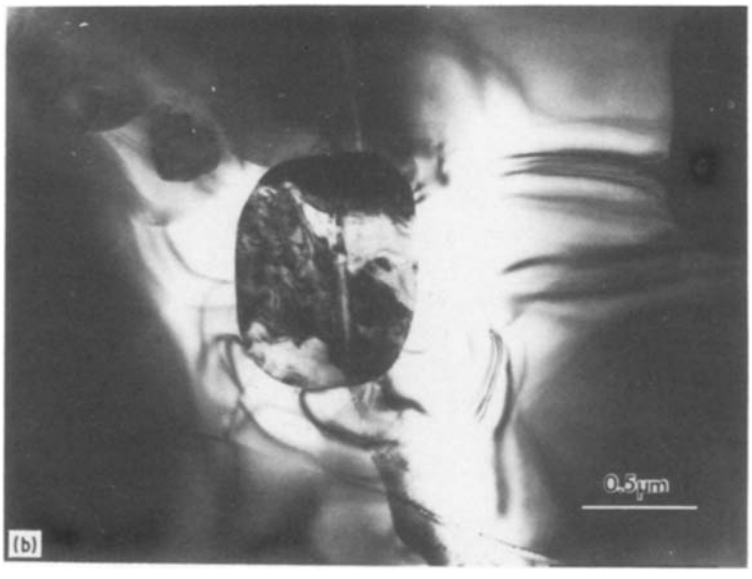

Figure 2 Transmission electron micrographs of MgO-sample treated at 1450° C for 1.5 h which show: (a) microtwinned monoclinic intergranular-ZrO_2 grains and a mullite grain with low-angle grain-boundary dislocations (arrows), and (b) monoclinic intragranular-ZrO_2 grain and the stress lines due to the t-ZrO_2 → m-ZrO_2 transformation.

orientations with respect to the electron beam are noted, mainly: $\{1\,1\,0\}$, $\{0\,1\,0\}$, $\{1\,0\,1\}$, $\{\bar{3}\,1\,1\}$, $\{\bar{1}\,1\,\bar{1}\}$, $\{3\,\bar{1}\,3\}$. Transitory amorphous or glassy phase closer to these crystals (Fig. 4) has a composition of (wt %) 14.8 CaO, 33.4 Al_2O_3, 48.4 SiO_2, 3.4 ZrO_2 and coexists locally with zircon and zirconia. These glassy phases frequently show some radiation damaged produced by the electron beam.

Also during the reaction-sintering process in the two compositions studied, another kind of amorphous phase was found as thin foils at grain boundaries. These amorphous phases show the following compositions (wt %): 3.2 CaO; 72.3 Al_2O_3; 21.2 SiO_2; 3.3 ZrO_2 and 5.9 MgO, 68.9 Al_2O_3, 24.2 SiO_2; 1.1 ZrO_2 for CaO and MgO samples, respectively (Fig. 7).

The viscosity value of these phases, which have an Al_2O_3/SiO_2 ratio similar to that of mullite, estimated by the Vogel-Fulcher-Tamman equation [7] used in determining the glass viscosity, is higher than $\sim 10^{18}$ dPa sec. Because this value indicates that the analysed phase is not a glass, it will not correspond to the real viscosity because the mentioned equation would not be adequate in this case. This phase could be amorphous, similar to that observed by Di Rupo and Anseau [8] in $ZrSiO_4/Al_2O_3$ mixtures treated at 1450° C.

In the CaO-containing sample heated at 1450° C, 2 h, small glassy-phase pockets at triple points were detected with the following composition (wt %): 15.5 CaO; 36.5 Al_2O_3, 43.0 SiO_2 and 6.0 ZrO_2 which is

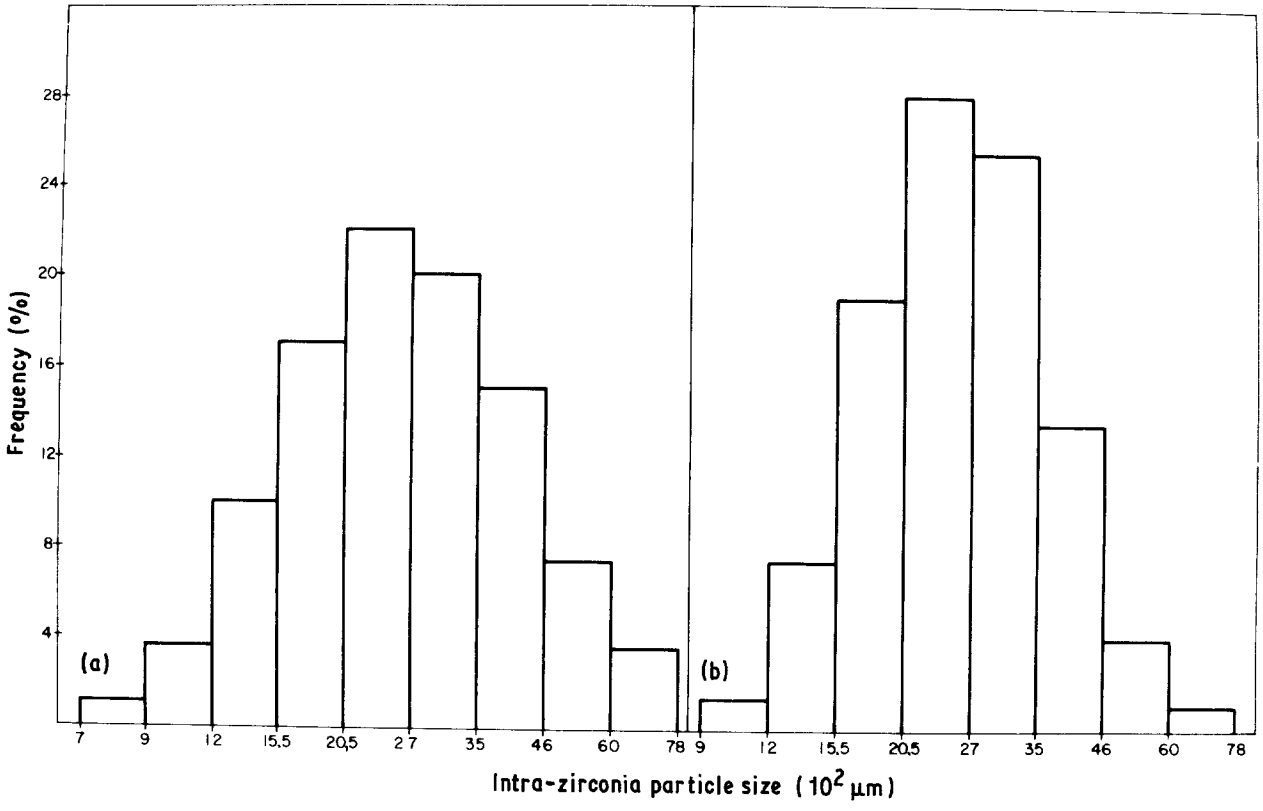

Figure 3 Intragranular-ZrO_2 particle size distributions. (a) CaO sample treated at 1450° C for 2 h, d = 0.30 (0.08) μm. (b) MgO sample treated at 1450° C for 1.5 h, d = 0.29 (0.07) μm.

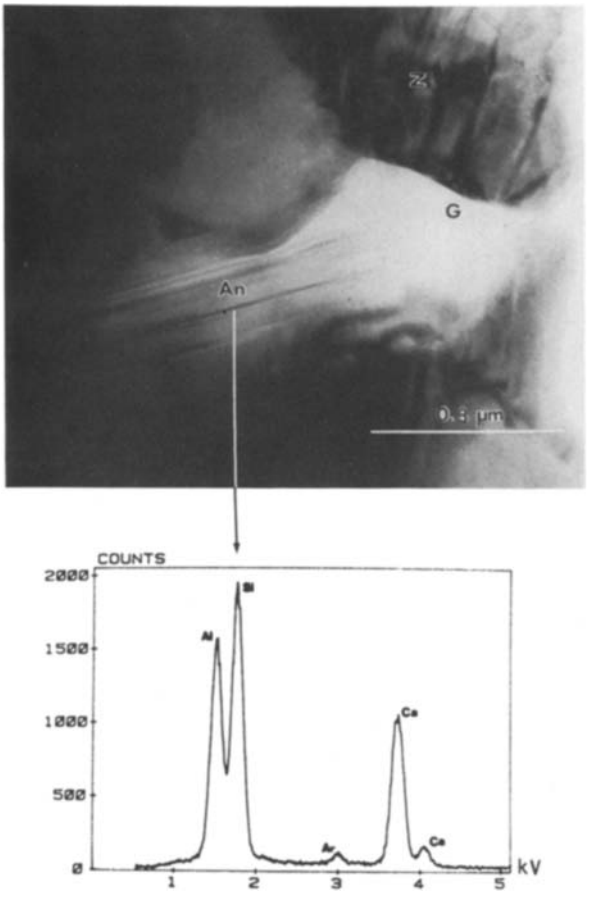

Figure 4 Transmission electron micrograph corresponding to a CaO sample treated at 1425° C for 17 h showing an anorthite crystal (An) nucleating inside the glassy phase (G) and its EDX spectrum. Z = ZrO_2.

close to that of the ZrO_2–Al_2O_3–mullite–anorthite peritectic of the Al_2O_3–SiO_2–ZrO_2–CaO system [3].

In the MgO-containing sample treated at 1450° C, 1.5 h such kind of liquid phase was not observed, probably due to the fact that the corresponding peritectic point is located at 1450° C [4].

The results obtained in the present work clearly indicate that the reaction sintering starts with the formation of anorthite (Fig. 4) or saphirine and spinel (Fig. 6) in the CaO- or MgO-containing samples, respectively, and the simultaneous decomposition of zircon. The local coexistence of anorthite, zircon and zirconia or saphirine, spinel and zirconia at the

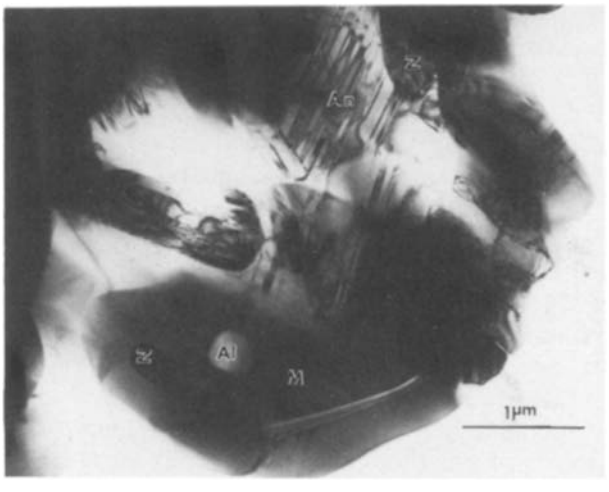

Figure 5 Transmission electron micrograph of a CaO sample heat treated at 1450° C for 2 h showing twinned anorthite crystals. Al = Al_2O_3.

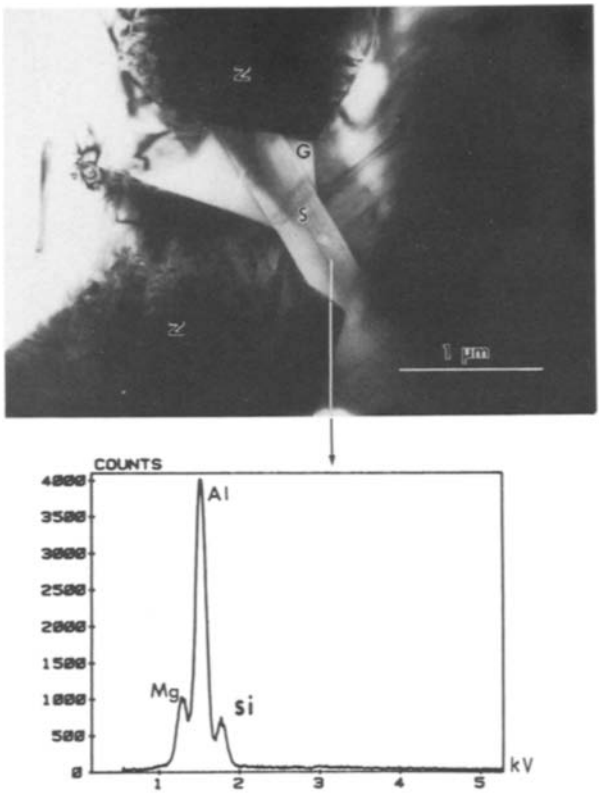

Figure 6 Transmission electron micrograph corresponding to an MgO sample treated at 1425° C for 17 h showing a saphirine crystal (S) and its EDX spectrum.

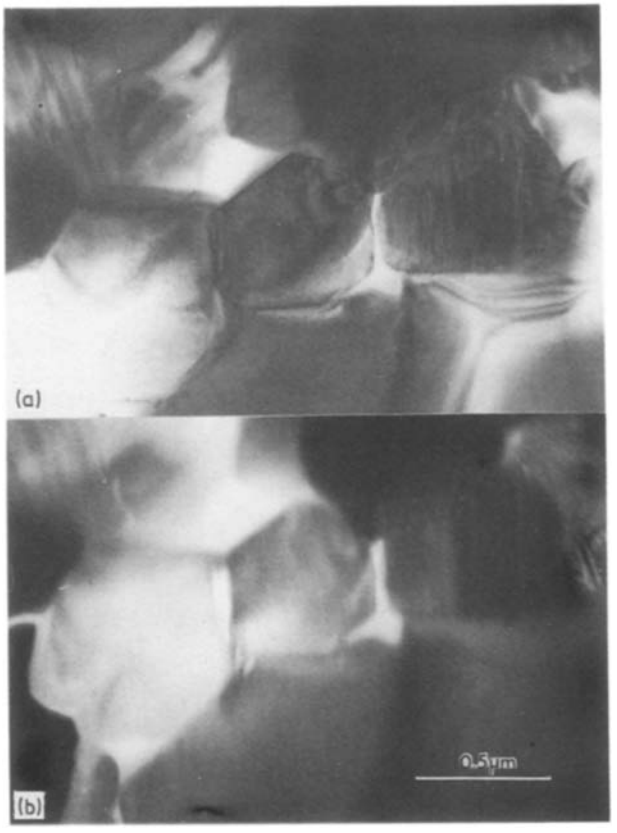

Figure 7 Amorphous grain-boundary phase in a CaO-sample heated at 1425° C for 17 h. (a) Shows a bright-field image in which the grains and the amorphous phase are clearly visible; (b) is a dark-field image taken with a part of the diffuse scattering caused by the amorphous ring. The amorphous areas show bright contrast.

appropriate temperature leads to the formation of a liquid phase corresponding to the lowest invariant point of the ZrO_2–Al_2O_3–SiO_2–CaO or ZrO_2–Al_2O_3–SiO_2– MgO systems [3, 4]. This liquid can diffuse by capillarity between the different grains enhancing the mass transport and consequently increasing the sintering reaction rates up to its final disappearance when the chemical equilibrium is reached at the corresponding sintering temperature. When the temperature of sintering is $\geqslant 1450°$ C a small amount of permanent glassy phase with a composition close to the peritectic points remains at triple points.

The mullite grains grow trapping ZrO_2 particles and some alumina grains. The intergranular microtwinned ZrO_2 grains have larger average grain size than the intragranular ZrO_2 grains due to the fact that the mass transport takes place through a liquid phase as observed in Figs 1, 2, 4 and 5.

Table I shows the mechanical properties as well as the t-ZrO_2 content for the two samples studied and for a mullite/ZrO_2 composite obtained by conventional sintering [9]. Although flexural strength values are quite similar for all samples, critical stress intensity factor values in the mullite/ZrO_2 composites obtained by reaction sintering are significantly higher than that corresponding to conventional sintered mullite/ZrO_2 composite. The increase in toughness for this last composite has been explained elsewhere considering the following two mechanisms: transformation toughness and toughening by the presence of solid solution at the grain boundary [10]. Because the t-ZrO_2 content and the solid solution range are similar for both kinds of mullite/ZrO_2 composites [10], an additional toughening mechanism must be considered.

Microcracks starting from the monoclinic-ZrO_2 grains have frequently been observed by TEM in CaO- and MgO-containing samples (Fig. 8). Although these microcracks could be produced during the TEM test, it may indicate a tendency of the material to form microcracks. This was not observed in conventionally sintered mullite/ZrO_2 composites. On the other hand, flexural strength has practically the same value for both kinds of mullite/ZrO_2 composites, and therefore the critical flaw size is lower in the sintered composite. All these facts suggest that the increase in toughness observed in the reaction-sintered composites compared with the sintered one seems to be related to a microcracking mechanism.

TABLE I Tetragonal ZrO_2 content and mechanical properties of mullite/ZrO_2 composites

Composite	T(° C)	t(h)	t-ZrO_2 (%)	σ_f(MPa)	K_{IC}(MPa m$^{1/2}$)
Mullite/ZrO_2/anorthite	1450	2.0	4.0	235 ± 30	4.3 ± 0.1
Mullite/ZrO_2/spinel	1450	1.5	4.0	258 ± 26	4.46 ± 0.05
Mullite/ZrO_2	1570	2.0	4.4	253 ± 20	3.0 ± 0.1

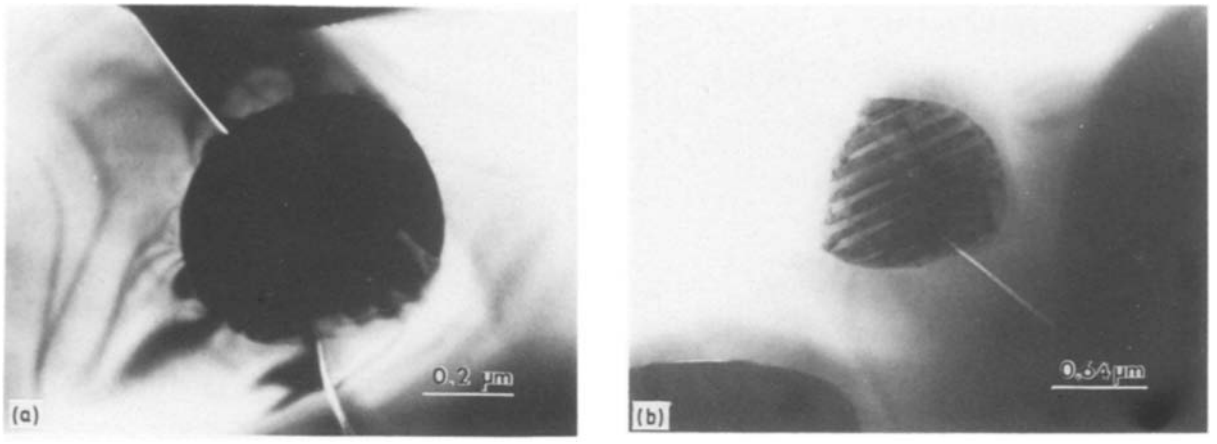

Figure 8 Radial microcracking in the surroundings of m-ZrO_2 particles observed in: (a) an MgO sample heated at 1450° C for 1.5 h, and (b) a CaO sample treated at 1450° C for 2 h.

4. Conclusions

Two kinds of transitory amorphous phases have been noted in both CaO- and MgO-containing compositions: (a) a silica-rich glassy phase located at triple points and (b) an amorphous thin foil at the grain boundaries with a composition very close to that of mullite.

Two kinds of zirconia particles were observed in both reaction-sintered compacts: (a) intragranular round ZrO_2 particles with an average diameter of $\sim 0.3\,\mu m$ and (b) intergranular sharp-edged ZrO_2 particles with an average grain size of $\sim 1.3\,\mu m$.

A small amount of permanent glassy phase with a composition close to the corresponding peritectic point, was observed only in CaO samples heated at 1450° C. This glassy phase is located in the neighbourhood of intergranular ZrO_2 and anorthite grains. The mullite–mullite grain boundary was generally glass free, showing low-angle grain-boundary dislocations.

Solid solutions of Al_2O_3 and SiO_2 in ZrO_2 grains, as well as ZrO_2 in mullite grains, have been measured. CaO and MgO solid solutions in ZrO_2 grains have not been detected.

The increase in toughness observed in both reaction-sintered composites seems to be related to a microcracking mechanism.

Acknowledgements

The authors thank CAICYT (Spain), Ref. N 560 and the Director, Office of Energy Research, Office of Basic Energy Sciences. Materials Science Division of US DOE no. DE-AC03-76SF00098, for support.

References

1. N. CLAUSSEN and J. JAHN, *J. Am. Ceram. Soc.* **63** (1980) 228.
2. M. R. ANSEAU, C. LEBLUD and F. CAMBIER, *J. Mater. Sci. Lett.* **2** (1983) 366.
3. P. PENA, P. MIRANZO, J. S. MOYA and S. DE AZA. *J. Mater. Sci.* **20** (1985) 2011.
4. P. MIRANZO, P. PENA, J. S. MOYA and S. DE AZA, *ibid.* **20** (1985) 2702.
5. P. PENA and S. DE AZA, "Advances in Ceramics", Vol. 12, edited by N. Claussen and M. Rühle (American Ceramic Society, 1984) p. 174.
6. G. CLIFF and G. W. LORIMER, *J. Microscopy* **103** (1975) 203.
7. H. SCHOLZE, "Le Verre. Nature, Structure et Propriétés" (Institut du Verre, Paris, 1980) p. 142.
8. E. Di RUPO and M. R. ANSEAU, *J. Mater. Sci.* **15** (1980) 114.
9. J. S. MOYA and M. I. OSENDI, *J. Mater. Sci. Lett.* **2** (1983) 599.
10. M. I. OSENDI, P. MIRANZO and J. S. MOYA, *ibid.* **4** (1985) 1026.

Received 7 October 1986
and accepted 20 January 1987